



**FORMULATION DEVELOPMENT, OPTIMIZATION,
EVALUATION, AND STABILITY STUDIES OF NIOSOMES**

Vaibhav L Narwade*¹ Dr. Namrata Singh²

1. Research Scholar, Department of Pharmaceutics, Oriental University Indore, MP, India

2. Professor, Faculty of Pharmacy, Oriental University Indore, MP, India

**Corresponding author: Vaibhav Laxmikant Narwade*

(Ph D. Scholar Oriental University, Indore, M.P)

Email id: vaibhavnarwade49@gmail.com

Contact No: 9511762800

Running Title: Formulation and Evaluation Niosomes.

Abstract

The niosomes are organized using thin-film hydration and sonication techniques. For the film hydration method, dissolve surfactant, cholesterol, stearylamine (65.0:30.0:5.0 mM) and captopril (2 mg) in aggregates containing chloroform:ethanol (3: 1).

The solvent was evaporated under vacuum on a rotary evaporator to form a thin film. Using a stirrer, replace the membrane then hydrate with 10 mL of phosphate buffer (pH 7.4). For ultrasonic techniques, surfactants, cholesterol, stearylamine (65.0:30.0:5.0 mM) and captopril (2 mg) were mixed in a beaker, and 10 ml of phosphate buffer (pH 7.4) was added. I left it for five hours. White dispersions (niosomes) were synthesized 7 min before sonication as needed.

In the ether injection technique, a solution containing a mixture of ether and surfactant is introduced slowly into an aqueous solution (preheated to 60°C) to evaporate the ether and synthesize a milky paste. The products were thus analyzed for a number of parameters, including percent encapsulation efficiency, vesicle length, polydispersity index, and zeta capacity, and were determined to be state-of-the-art. technology for making niosomes based on this specification.

Introduction

The transdermal drug delivery process offers many advantages for adjacent drug delivery and systemic therapy. However, skin is often misdiagnosed for its strong barrier properties compared to other biofilms due to the impermeable nature of the stratum corneum. Due to the low permeability of the skin, the drug entry point is small. Various drug delivery modules are available to increase the permeability of molecules. b.

Energetic and passive devices including iontophoresis, phonophoresis, penetration enhancers and other drug delivery modules. Vesicular delivery of the drug may be beneficial because the vesicles tend to fuse together and adhere to the moving bed, primarily due to the excellent permeability of the drug at the interface of the pores and the stratum corneum of the skin. It is believed to increase thermodynamic activity. These vesicles act as drug depots. Surface charges on the vesicles can modulate the rate of drug release at the target site.

The surface charge of vesicles is usually assessed by measuring the zeta potential. It provides data on the general grounding rate of particles and the consequences of environmental changes, and through the steady efforts of formulators, increasingly complex drug delivery structures are designed. The scientific goals are to broaden structure, minimize side effects, provide long-term therapeutic benefits at lower doses, reduce frequency of administration, and improve patient compliance.

Optimization of formulation ingredients

Generation of niosomes in different batches using current and type switching of nonionic surfactants. Therefore, after selecting the optimized formulation, the obtained products were analyzed for various indicators such as polydispersity index, zeta strength, vesicle length and encapsulation efficiency.

Materials and Method

Formulation and evaluation of niosomes

Niosomes are capable of entangling a wide variety of medicine. They include non-ionic stearylamine, LDL cholesterol, and surfactants.

Selection of nio somes method of preparation

Nio somes were synthesized by different methodologies

1. Ether injection Technique
2. Thin film hydration Technique
3. Sonication Technique

The formulation was analyzed for the vesicle size, polydispersity index, zeta potential, and entrapment efficiency, the result of which are listed in Table 1.

Table 1: Optimization of method for niosome preparation

Code	Method of preparation	Vesicle size in (nm)	PDI	Zeta potential (mV)	%EE
F1	Ether injection method	715.0 ± 6.4	0.357	-34 ± 4.7	83.3 ± 3.14
F2	Film hydration method	524.0 ± 3.8	0.345	-37 ± 9.3	85.1 ± 2.15
F3	Sonication method	299.5 ± 2.1	0.254	-45.5 ± 9.3	92.1 ± 3.4

Span60: Cholesterol:Stearylamine:65.0:30.0:5.0mM, Captopril:2mg, Polydispersity Index:PDI, Entrapment efficiency: EE, Millivolts:mV

Optimization of formulation ingredients

Niosome preparations were prepared by the sonication method with varying concentrations of nonionic surfactant, cholesterol, and captopril, as shown in Table 2, and analyzed for vesicle size, polydispersity index, zeta potential, trapping efficiency, etc. were evaluated for various parameters.

Table2: Optimization of niosome composition

Code	Concentration(mM)			Risp (mg)	Vesicle size(nm)	PDI	Zeta potential (mV)	%EE
	Sp60	Ch	SA					
C1	30.0	65.0	5.0	2	202.7 ± 6.7	0.309	-37.3 ± 6.48	48.3 ± 3.01
C2	47.5	47.5	5.0	2	269.4 ± 7.1	0.161	-39.7 ± 5.35	65.70 ± 2.8
C3	55.0	40.0	5.0	2	207.2 ± 5.7	0.243	-39.5 ± 6.84	79.89 ± 3.4
C4	65.0	30.0	5.0	2	238.1 ± 3.2	0.256	-45.0 ± 8.35	92.83 ± 2.4
C5	65.0	30.0	5.0	5	242.3 ± 4.5	0.234	-46.0 ± 8.35	94.36 ± 5.7
C6	65.0	30.0	5.0	10	245.7 ± 6.5	0.248	-45.6 ± 8.35	95.83 ± 6.1

Span60:Sp60,Cholesterol:Ch,Stearylamine:SA,Millimoles:mM,PolydispersityIndex:PDI,
Entrapmentefficiency:EE, Millivolts:mV

Continuous efforts are developing increasingly sophisticated drug delivery systems. Niosomes containing different kinds of surfactants were also synthesized by sonication technique and analyzed for vesicle size, zeta potential, polydispersity index and trapping efficiency. These are listed in Table 3.

Table3:Selection of surfactant for niosomes

Formulation Code	Composition (mM) 65.0:30.0:5.0	Vesiclesize (nm)	PDI	ZetaP otential (mV)	%EE
S1	Sp20:Ch:SA	232.0 ± 7.5	0.171	-24.0 ± 3.76	74.5 ± 5.3
S2	Sp40:Ch:SA	219.1 ± 3.4	0.277	-40.1 ± 7.79	90.01 ± 4.2
S3	Sp60:Ch:SA	213.9 ± 3.1	0.269	-50.6 ± 9.31	92.83 ± 3.4
S4	Sp80:Ch:SA	290.2 ± 4.3	0.209	-35.4 ± 3.96	78.5 ± 2.35
T1	Tw20:Ch:SA	388.9 ± 8.8	0.350	21.9 ± 4.62	62.31 ± 3.9
T2	Tw40:Ch:SA	258.7 ± 7.3	0.437	21.3 ± 3.83	70.87 ± 4.2

T3	Tw60:Ch:SA	248.2 ± 7.5	0.427	20.4 ± 4.31	72.47 ± 5.3
T4	Tw80:Ch:SA	180.0 ± 8.7	0.389	25.1 ± 3.74	68.62 ± 3.1

Span:Sp, Cholesterol:Ch, Stearylamine:SA, Millimoles:mM, Polydispersity Index:PDI, Entrapment efficiency:EE, Millivolts:mV, Tween:Tw

Result and Discussion

a. Entrapment efficiency(%EE)

Formulation number S3 showed the highest entrapment efficiency ($92.83 \pm 3.4\%$) and was found in the order of Span60 > 40 > 80 > 20 which could be due to its structure, 3-dimensional orientation, and behavior of its surfactants

Span60 (lower HLB 4.7) seems to be the best carrier with good efficiency of entrapment than Span20 and Span40 (HLB 8.6 and 6.7).

b. Vesicle size, zeta potential, and polydispersity index

Niosomes synthesized using Span60 have the smallest vesicle size. This may be due to the low HLB. Excessive zeta potentials in all cases (Figure 1) reflected that the formulations were potent, and the reduction in PDI confirmed that the formulations were homogenous.

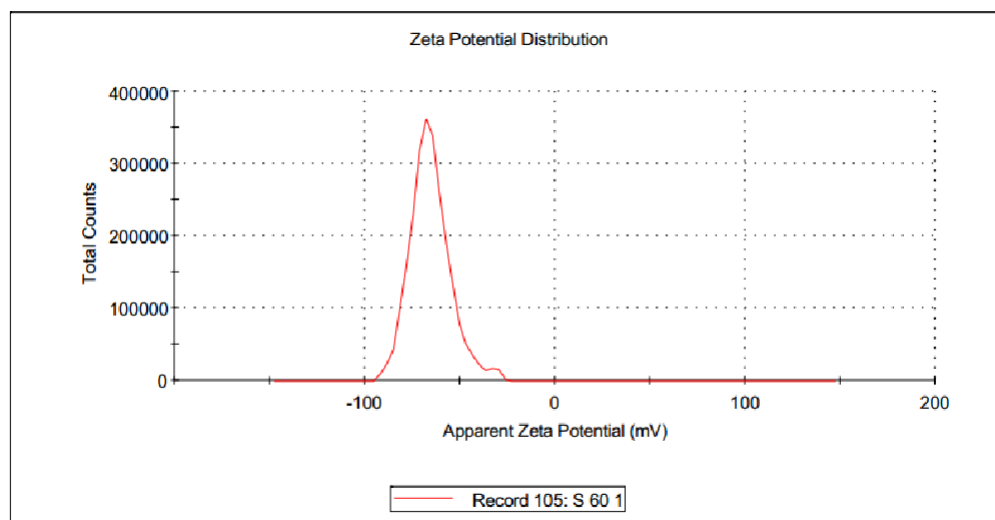


Fig1: Zeta potential of Captopril niosomes with Span60

- c. Niosomes with an interval of 60 had the best adhesion performance ($92.83 \pm 3.4\%$). Selected formulations were chosen for further evaluation because the *in vivo* performance of niosomes depends on the amount of drug loaded into the niosomes.

In-vitro release study

Figure 2 shows the cumulative drug release profile of captopril from the niosome formulation. This indicates that the release of captopril from the niosomes is rapid and slow during the first hour compared to the release rate of captopril API (suspension). About 98% of the drug was released from the captopril drug suspension within 6 hours, while only 29% was released from the niosomes. Top 20 team (88.36%).

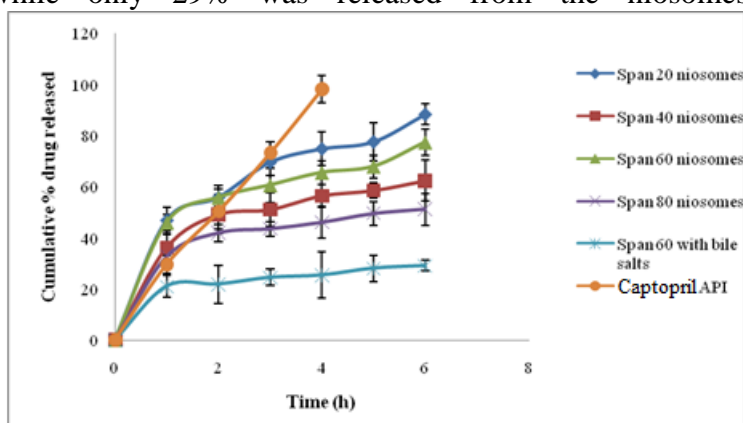


Fig2: *In-vitro* release study of Captopril from niosomes

d. Stability studies of niosomes in presence of bile salts

Preparations of niosomes containing different groups of species were incubated with 0, 2.5, 5, 7.5, 10, 15 and 20 mM sodium deoxycholate solutions at 37°C for 1 h, and the effect was measured using a turbidimeter. Analysis and evaluation (Figure 3).

From Figure 16, it can be seen that the turbidity above 10 mM drops sharply with kilometers due to the solubility of the bilayer. The Span60 formulation did not significantly reduce haze. This is due to the high cutting transition temperature (Table 4). The Span60 formulation exhibited the highest turbidity even after the release of 20 mM sodium deoxycholate, confirming the structural tension of the niosome bilayer. The low turbidity of the Span20 and Eighty formulations is due to their fluidity, which allows a smooth transition from bilayer to micellar form.

Table4:Effect ofbilesaltson niosomes containingdifferent typesof span

Sodium desoxycholate (mM)	Turbidity(NTU)			
	Span20	Span40	Span60	Span80
0	500	500	500	500
2.5	482	490	492	411
5	441	465	484	372
7.5	423	452	471	331
10	407	431	460	309
15	258	339	433	181
20	159	283	363	103

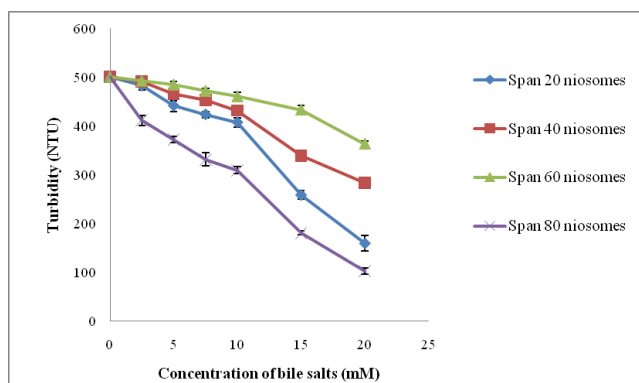


Fig 3: Effect of bile salts on niosomes containing different types of span

Table 5: Effect of bile salts on niosomes containing bile salts as an integral component

Sodiumdesoxycholate (mM)	Turbidity (NTU)				
	Span60 (0mM)	Span60 (2.5mM)	Span60 (5mM)	Span60 (7.5mM)	Span60 (10mM)
0	500	500	500	500	500
2.5	485	494	496	498	495
5	474	487	488	490	486
7.5	455	478	480	486	476
10	420	462	467	470	445

15	400	430	440	460	419
20	363	410	435	452	380

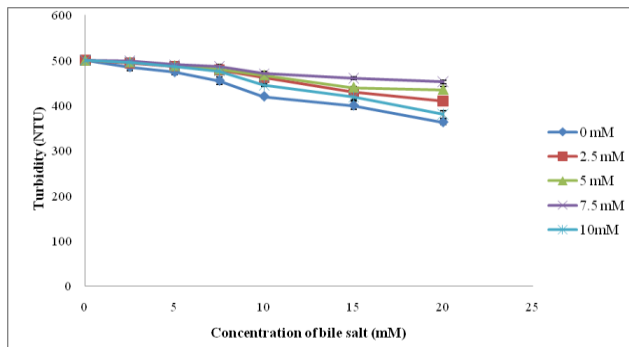


Fig 4: Effect of bile salts on niosomes containing bile salt as integral components

e. Morphology

The morphological properties of niosomes (S3) were observed by transmission electron microscopy. TEM photomicrograph of lyophilized niosomes is shown in Fig 5,

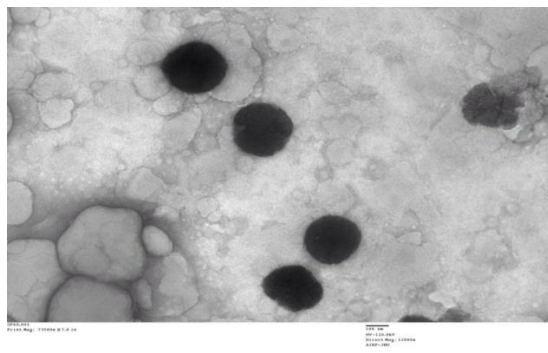


Fig 5: Transmission electron photomicrograph of Captopril niosomes

f. Drug-excipient compatibility studies

Drug-excipient compatibility studies were performed using infrared spectroscopy and differential scanning calorimetry.

Drug-excipient compatibility study using FTIR spectroscopy

FTIR spectra of captopril, Span60, aggregates (1:1), empty niosome and charged niosome

of captopril are shown in Figure 2. N-H bent), 1128 cm⁻¹ (C-H stretched), 853 cm⁻¹ (C-H bent, aromatic) and 3744 cm⁻¹ (N-H stretched). Span60 is 1200 cm⁻¹ (aliphatic), 1734 cm⁻¹ (five-membered cyclic ring), 1400 cm⁻¹ (-CH₃), 2928 cm⁻¹ (aliphatic C-H stretch, not equal), 2800 cm⁻¹ (aliphatic relative ring) C-H-root), symmetric) and 3400 cm⁻¹ (O-H stretch).

Analysis of the physical mixture of captopril and Span60 showed the presence of characteristic captopril peaks in the physical mixture similar to the individual captopril spectra, no detectable changes in the FTIR spectra, and no chemical differences between them. Indicates that no significant interaction was found. His FTIR spectra of empty and captopril-loaded niosomes showed weak interactions between cholesterol and Span60 in the 3600 cm⁻¹ and 3200 cm⁻¹ wavenumber regions. Between N-H, C=O, -OH and other functional groups, van der Waals force, dipole moment, etc. Leads to the formation of hydrogen bonds and other weak bonds.

However, these interactions may promote the formation of the vesicle shape, thereby stabilizing the structure and delaying drug release. Formation of hydrogen bonds between membrane components of niosomes and its impact on encapsulation efficiency and slowed drug release.

Fig 6: IR spectra(a) Captopril (b) Span 60 (c) physical mixtures (d) blank niosomes (e) Captopril loaded niosomes

Drug-excipient compatibility take a look at the usage of differential scanning calorimetry (DSC)

The thermal transition of captopril occurs at 174°C, which corresponds to its melting point, and it exhibits a sharp endothermic peak at this temperature. Span 60 exhibits an endothermic peak at 59.32°C, and the disappearance of this peak is shown in Figure 3. 20b and 20c are due to cholesterol forming a bilayer.

Wilke et al. Using molecular modeling studies and thermal analyses, we have shown that during the formation of the niosome bilayer, cholesterol is embedded between surfactant molecules, resulting in rigidity of the vesicles.

g. Drug release kinetics

The release of captopril from the niosomes followed the Korsmeyer-Peppas model (Table 6). For n values less than 0.5, the release of captopril follows a Fick diffusion mechanism. H. Drug release occurs through a chemical potential gradient from high to low concentration due to molecular diffusion.

The Korsmeyer-Peppas model also indicates several concurrent processes such as B. Diffusion of water into the drug reservoir, drug swelling, gelation, and leaching during absorption.

Table 6: Drug release kinetics of the optimized formulation

Release-Kinetics	Zero order		First order		Higuchi Model		Korsmeyer Peppas's model	
	K	r ²	K	r ²	K	r ²	n	r ²
	5.6782	0.9668	0.0406	0.9424	19.816	0.9725	0.2679	0.9759

h. Stability studies (at different temperatures)

The stability of the Niosome was evaluated under different temperature conditions (4 ± 1 °C and 25 ± 2 °C). He analyzed the formulation for 3 months and observed no visual changes in the niosome formulation. The results are shown in Table 7.

Table7: Effect of temperature on niosome formulations

Temperature	Time-interval (days)	Parameters		
		Appearance	Vesicle-Size (nm)	Entrapment-efficiency(%)
Refrigeration ($4 \pm 1^\circ\text{C}$)	0	No-change	299 ± 0.1	85
	45	No-change	308 ± 1.2	80
	90	No-change	315 ± 3.6	79.8
Room temperature ($25 \pm 2^\circ\text{C}$)	0	No-change	299 ± 0.1	85
	45	No-change	312 ± 2.8	83
	90	No-change	322 ± 2.1	78.97

The niosome capture efficiency did not change significantly between $4 \pm 1^\circ\text{C}$ and $25 \pm 2^\circ\text{C}$. Encapsulation efficiency was slightly reduced, possibly due to drug leakage from the vesicles. Stability studies showed that the niosome formulation was more stable at $4 \pm$

1°C than at $25 \pm 2^\circ\text{C}$.

Ex-vivo absorption studies

Non-inverse and inverse Ratsack techniques have been used to assess mechanisms of drug transport in the gut. This helps predict the in vivo absorption profile of the formulation in humans. Compared to the inverted sac method, the non-inverted sac model has the following advantages: Therefore, we used the non-inverted sac method to assess isolated intestinal permeability. Table 8 shows the hydraulic conductivity, flux and amplification of the formulations. The expansion rate of niosomes (without bile) was greater than that of niosomes containing bile.

Table8: Ex-vivo intestinal permeation study and the permeability details

Formulation	Flux ($\mu\text{gcm}^{-2}\text{h}^{-1}$)	Permeability coefficient	Enhancement ratio
Control	66.85	0.5571	1
S-60niosomes	139.459	1.1607	2.08
S-60niosomeswith bile	89.078	0.7423	1.33

Summary and conclusion

The niosomes were prepared using the technique of ether injection, thin layer hydration and sonication, and sonication, which resulted in a homogeneous formulation with high entrapment efficiency. At a ratio of 65:30:5 mM (Span60: cholesterol: stearylamine), its Span60 formulation achieved the highest encapsulation efficiency of 92.83%. All niosome formulations show low polydispersity indices and high zeta potential values, which guarantee the stability and homogeneity of the formulation. FTIR studies ensure that there are no drug incompatibilities.

H. Captopril and formulation additives. It promotes the formation of vesicles, stabilizes the structure and slows the release of active ingredients. DSC data also supports these findings. The formulation was more stable at low temperature ($4 \pm 1^\circ\text{C}$), and no

significant change in vesicle size and encapsulation efficiency was observed.

References:

1. Van- Schaick EA, Lechat P, Remmerie BM. Pharmacokinetic comparison of fast-disintegrating and conventional tablet formulations of risperidone in healthy volunteers. *Clin Ther* 2003;25(6):1687-99.
2. Samuel K. Advances in psychotropic formulations. *Prog Neuropsychopharmacol Biol Psychiatry* 2006;30:996-1008.
3. Rainer MK. Risperidone long-acting injection: a review of its long term safety and efficacy. *Neuropsychiatr Dis Treat* 2008;4(5):919-27.
4. Biju SS, Talegaonkar S, Mishra PR, Khar RK. Vesicular systems: an overview. *Indian J Pharm Sci* 2006;68(2):141-53.
5. Hua S. Lipid-based nano-delivery systems for skin delivery of drugs and bioactive. *Front Pharmacol* 2015;6:1-5.
6. Verma P, Pathak K. Therapeutics and cosmeceutical potential of ethosomes: an overview. *J Adv Pharm Technol Res* 2010;1(3):274-82.
7. Udupa N. Niosomes as Drug Carriers. In: Jain NK, editors. *Controlled and Novel Drug Delivery*. India: CBS Publishers and Distributors; 1997, p.292-303.
8. Vyas and Khar, Targeted and controlled drug delivery- Novel Carrier Systems, CBS Publishers and Distributors, New Delhi, First edition reprint 2004, 249-279.
9. Mahale NB, Thakkar PD, Mali RG, Walunj DR, Chaudhari SR. Niosomes: novel sustained release non-ionic stable vesicular systems- an overview, *Adv Colloid Interface Sci* 2012;183:46-54.
10. Kumar GP, Rajeshwarao P. Non-ionic surfactant vesicular systems for effective drug delivery- an overview. *Acta Pharma Sin B* 2011;4:208-19.
11. Uchegbu IF, Double JA, Turton JA, Florence AT. Distribution, metabolism and tumoricidal activity of doxorubicin administered in sorbitan monostearate (Span 60) niosomes in the mouse. *Pharm Res* 1995;12(7):1019-24.
12. Yoshioka T, Sternberg B, Florence AT. Preparation and properties of vesicles (niosomes) of sorbitan monoesters (Span 20, 40, 60, and 80) and

- sorbitantrimester(Span85). Int J Pharm 1994;105(1):1-6.
13. Uchegbu IF, Vyas SP. Non-ionic surfactant-based vesicles (niosomes) in drug delivery. Int J Pharm 1998;172(1):33-70.
 14. Aungst BJ. Novel formulation strategies for improving the oral bioavailability of drugs with poor membrane permeation or pre-systemic metabolism, J Pharm Sci 1993;82(10):979-87.
 15. Aungst BJ. Enhancement of intestinal absorption of proteins and peptides. J Control Release 1996;41:19-31.
 16. El-Barghouthi MI, Masoud NA, Al-Kafawein JK. Host-guest interactions of risperidone with natural and modified cyclodextrins: phase solubility, thermodynamics, and molecular modeling studies. J Incl Phenom Macrocycl Chem 2005;53:15-22.
 17. Ould-Ouali L, Noppe M, Langlois X, Willems B, Riele PT, Timmerman P, et al. Self-assembling PEG-p(CL-co-TMC) copolymers for oral delivery of poorly water-soluble drugs: a case study with risperidone. J Control Release 2005; 102:657-68.
 18. Mathot F, Beijsterveldt L van, Preat V, Brewster M, Arien A. Intestinal uptake and biodistribution of novel polymeric micelles after oral administration. J Control Release 2006; 111:47-55.
 19. Jug M, Becirevic-Lacan M. Screening of mucoadhesive microparticles containing hydroxypropyl-beta-cyclodextrin for nasal delivery of risperidone. Comb Chem High Throughput Screen 2007; 10:358-67.
 20. Lu Y, Tang X, Cui Y, Zhang Y, Qin F, Lu X. In-vivo evaluation of risperidone-SAIB in-situ system as a sustained release delivery system in rats. Eur J Pharm Biopharm 2008;68(2):422-29.
 21. Muthu MS, Singh S. Preparation and characterization of nanoparticles containing a typical antipsychotic agent, Nanomedicine 2007;2(2):233-40.
 22. Muthu MS, Singh S. Studies on biodegradable polymeric nanoparticles of risperidone: *in vitro* and *in vivo* evaluation, Nanomedicine 2008;3(3):305-19.
 23. Muthu MS, Rawat MK, Mishra A, Singh S. PLGA nanoparticle formulations of risperidone: preparation and neuropharmacological evaluation. Nanomedicine 2009,5(3):323-33.

24. Rahman Z, Zidan AS, Khan MA. Risperidone solid dispersion for orally disintegrating tablet: its formulation design and non-destructive methods of evaluation. *Int J Pharm* 2010; 400(1-2):49-58.
25. Aggarwal G, Dhawan S. Psychotropic drugs and transdermal delivery: an overview. *Int J Pharm Biol Sci* 2010; 1(2):1-12.
26. Heemstra LB, Finnin BC, Nicolazzo JA. The buccal mucosa is an alternative route for the systemic delivery of risperidone. *J Pharm Sci* 2010; 99(11):4584-92.
27. Rahman Z, Zidan AS, Khan MA. Non-destructive methods of characterization of risperidone solid lipid nanoparticles. *Eur J Pharm Biopharm* 2010; 76(1):127-37.
28. Amann LC, Gandal MJ, Lin R, Liang Y, Siegel SJ. *In-vitro-in-vivo* correlations of scalable PLGA-risperidone implants for the treatment of schizophrenia. *Pharm Res* 2010; 27:1730-37.
29. Patel S, Chavhan S, Soni H, Babbar AK, Mathur R, Mishra AK, et al. Brain targeting of risperidone-loaded solid lipid nanoparticles by the intranasal route. *J Drug Target* 2011; 19(6):468-74.
30. Selmin F, Blasi P, De Luca PP. Accelerated polymer biodegradation of risperidone poly(D,L-lactide-co-glycolide) microspheres. *AAPS Pharm Sci Tech* 2012; 13(4):1465-72.
31. Silva AC, Amaral MH, Gonzalez-Mira E, Santos D, Ferreira D. Solid lipid nanoparticles (SLN)-based hydrogels as potential carriers for oral transmucosal delivery of risperidone: preparation and characterization studies. *Colloids Surf B Biointerfaces* 2012; 93:241-8.
32. Kozielska M, Johnson M, Reddy VP, Vermeulen AN, Li Cheryl, Grimwood S, et al. Pharmacokinetic-pharmacodynamic modeling of the D₂ and 5HT_{2A} receptor occupancy of risperidone and paliperidone in rats. *Pharm Res* 2012; 29:1932-48.
33. Krishnamoorthy V, Verma PRP, Sen S. Formulation and evaluation of risperidone-mannitol solid dispersions. *Farmacia* 2012; 60(6):877-94.
34. Yardi S, Hitoshi S, Hidehisa T. Developing *in-vitro-in-vivo* correlation of risperidone immediate release tablet. *AAPS Pharm Sci Tech* 2012; 13(3):

890-95.

35. Bagratashvili VN, Egorov AM, Krotova LI, Mironov AV, Panchenko V Ya, Parenago OO, et al. Supercritical fluid micronization of risperidone pharmaceutical substance. *Russ J Phys Chem B* 2012;6(7):804-12.